Multigrain Platinum Nanowires Consisting of Oriented Nanoparticles Anchored on Sulfur-Doped Graphene as a Highly Active and Durable Oxygen Reduction Electrocatalyst

*Md Ariful Hoque, Fathy M. Hassan, Drew Higgins, Ja-Yeon Choi, Mark Pritzker, Shanna Knights, Siyu Ye, and Zhongwei Chen**

Proton exchange membrane fuel cells (PEMFCs) are attractive and promising clean operating devices to replace fossil fuel-based power technologies. The commercial adoption of PEMFCs is however still hindered by several critical issues[1] among which the design of highly durable cathode electrocatalysts for the oxygen reduction reaction (ORR) remains a formidable challenge.[2] As of now, the only practical catalyst technology used in PEMFC systems is based on platinum nanoparticles (2–5 nm) supported on carbon black (Pt/C). During PEMFC device operation, Pt nanoparticles are however susceptible to agglomeration/dissolution/Oswald ripening because of their high surface energies, which, along with the detrimental impact of carbon support corrosion, inevitably lead to radical performance degradation.[2b,3] Therefore, careful electrocatalyst design strategies must be applied to mitigate the inherent stability issues associated with both the Pt nanoparticles and the conventional carbon supports to achieve practical durability targets.[4]

Recently, 1D nanostructures such as Pt nanowires have been demonstrated capable of overcoming some of the drawbacks of Pt nanoparticles in catalyzing ORR, in particular, providing much improved catalytic activity and/or durability.[3a,5] The durability of Pt nanowires can be further improved by growing the nanowires onto stable nanostructured support materials, such as graphene or carbon nanotubes.[6] Unlike the carbon black conventionally used to support Pt catalysts, graphene in particular possesses very unique chemical, mechanical, and electrical properties due to its 2D sp^2 hybridized carbon network.[7] Studies have additionally shown that doping graphene with heteroatoms is an effective way to tune the intrinsic properties, which is beneficial for improving electrocatalyst activity and stability.[8] In our previous work, we demonstrated that sulfur-doped graphene (SG) is a highly promising support for Pt nanoparticles, providing a 14% increase in Pt-based mass activity in comparison to the state-of-the-art Pt/C and remarkable stability in terms of electrochemically active surface area (ECSA) and mass activity retention following accelerated durability testing (ADT).[9] We propose that combining the beneficial catalyst-support interactions provided by SG with Pt nanostructure control strategies (i.e., 1D nanowires) could provide further ORR activity and durability improvements to achieve practical targets for commercial devices.

Herein, we report the direct synthesis of Pt nanowires on SG (PtNW/SG) by applying a simple and facile surfactant-free solvothermal technique.[10] The prepared PtNWs are comprised of numerous single crystalline nanoparticles oriented along the <111> direction, and provide increased Pt-mass-based ORR activity in comparison to commercial Pt/C catalyst and PtNWs supported on graphene (PtNW/G). Most notably, PtNW/SG showed excellent stability through 3000 cycles of ADT in terms of both ECSA and ORR activity retention. By combining the advantages of both the 1D nanostructure of Pt and unique support materials, PtNW/SG are reported as a practical and highly promising candidate for overcoming the long term durability issues of conventional PEMFC cathode electrocatalysts.

SG with a sheet-like morphology (**Figure 1**a) was prepared and found by X-ray photoelectron spectroscopy to possess a surface sulfur content of 1.05 at%, consisting primarily of thiophenic species (Figure S1, Supporting Information). After the solvothermal synthesis of PtNW on the SG, the overall morphology of the materials is shown in Figure 1b. A variety of nanowire diameters ranging from 3 to 25 nm are observed, along with nanowire lengths in excess of 1 μm (Figure 1c). The crystal structure of Pt nanowires was confirmed to be Pt-fcc (JCPDS No. 04-0802) based on the X-ray diffraction (XRD) peaks shown in Figure S2 (Supporting Information), with diffraction patterns of commercial Pt/C and PtNW/G shown for reference. High-resolution transmission electron microscopy (HR-TEM) images of the Pt nanowires shown in Figure 1d indicate that the nanowires are composed of numerous attached Pt crystals oriented along the <111> direction, with a measured d-spacing of 2.24 Å corresponded to the (111) facet. Interestingly, Pt nanowires with different diameters possess the same

M. A. Hoque, Dr. F. M. Hassan, D. Higgins, J.-Y. Choi, Prof. M. Pritzker, Prof. Z. Chen
Department of Chemical Engineering
Waterloo Institute for Nanotechnology
Waterloo Institute of Sustainable Energy
University of Waterloo
200 University Ave. W, Waterloo ON N2L 3G1, Canada
E-mail: zhwchen@uwaterloo.ca
S. Knights, Dr. S. Ye
Ballard Power Systems, Inc.
9000 Glenlyon Parkway
Burnaby BC V5J 5J8, Canada

DOI: 10.1002/adma.201404426

ADVANCED MATERIALS
www.advmat.de

Materials Views
www.MaterialsViews.com

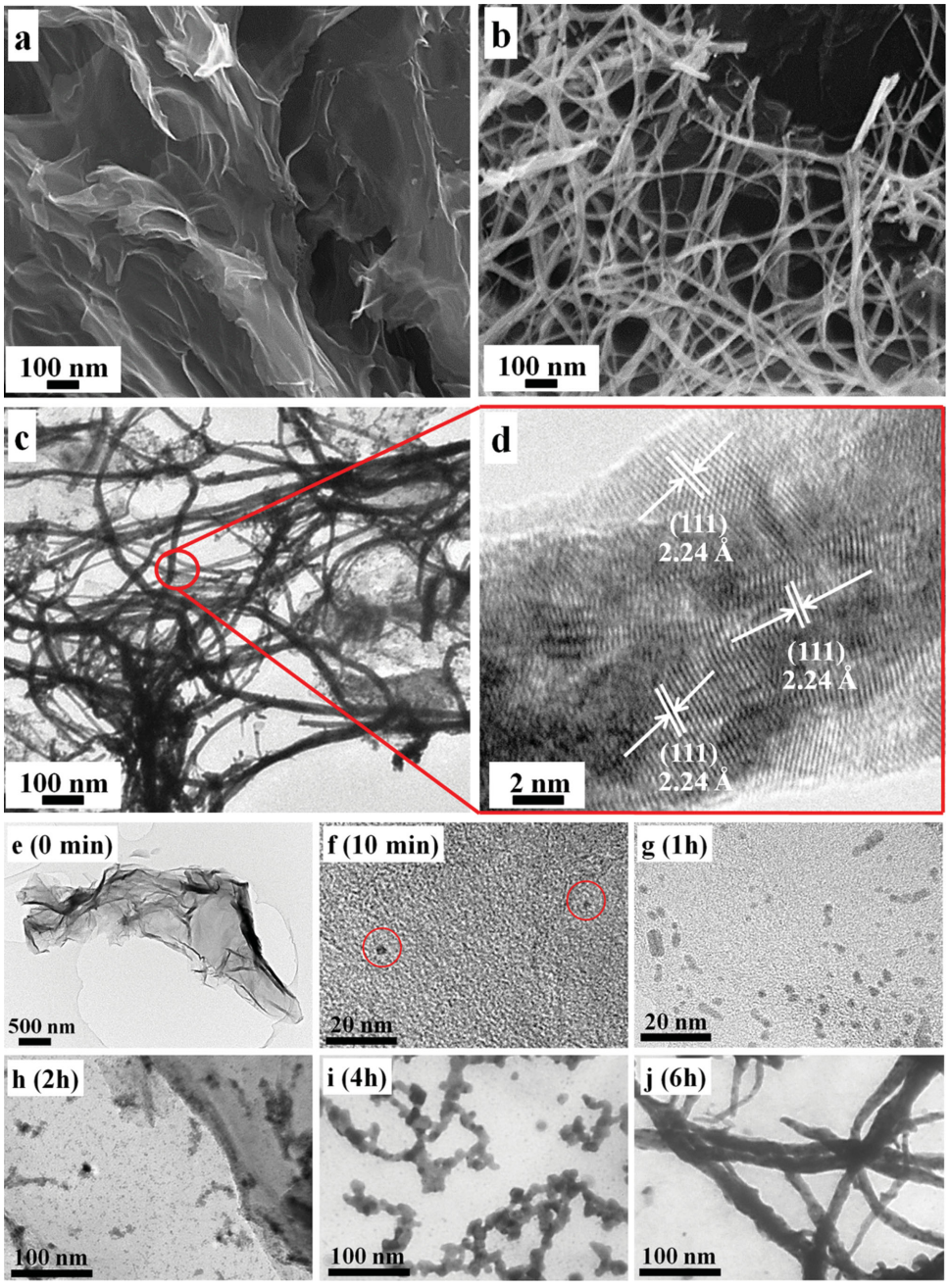

Figure 1. SEM image of a) SG and b) PtNW/SG. c) TEM image and d) HR-TEM image with d-spacing measurements of PtNW/SG. TEM images of PtNW/SG at different reaction durations of e) 0 min, f) 10 min, g) 1 h, h) 2 h, i) 4 h, and j) 6 h.

crystallographic orientation along the <111> direction as shown from a HRTEM image of a nanowire possessing a smaller diameter (ca. 7 nm) in Figure S3 (Supporting Information). For comparison, the structure of undoped graphene and PtNW/G are shown in Figure S4a,b (Supporting Information), respectively. We investigated the time-dependent growth mechanism of Pt nanowires on SG and the results are shown in Figure 1f–j. After just 10 min of reaction, growth is initiated by the nucleation of nano-sized Pt particles on the surface of SG (Figure 1f). After 1 h, the number of nanoparticles on SG increases significantly, and side-by-side attachment is observed (Figure 1g). Interestingly, after 2 h, the process of attachment and coalescence of nanoparticles eventually occurs to the point that nanorods are formed (Figure 1h). This process is continued with an increase in reaction time to 4 h, where it can be clearly seen in Figure 1i that the nanoparticles have attached together to form nanowires with larger lengths, and finally, after 6 h, smooth, continuous nanowires are obtained (Figure 1j). Based on these observations, it appears that the PtNWs evolve from the preferential attachment and crystallographic arrangement[11] along the <111> direction, rather than a seed-initiated growth process.[12]

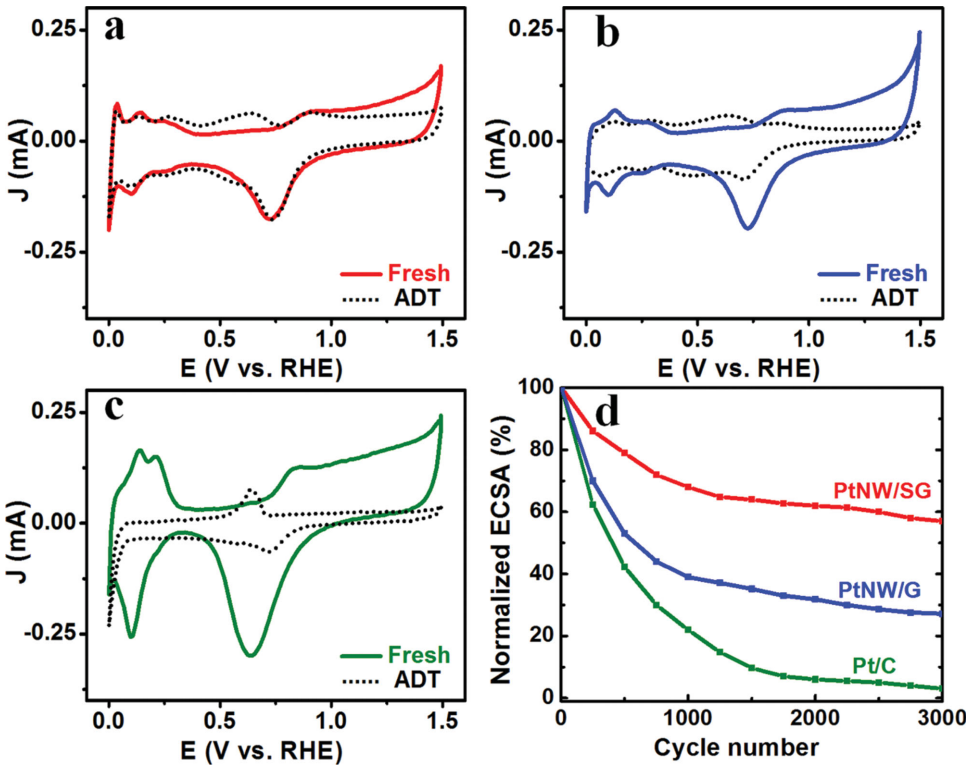

Figure 2. CV curves for a) PtNW/SG, b) PtNW/G, and c) Pt/C before and after ADT. d) Normalized ECSA values as a function of cycle number.

The electrochemical properties and stability of the various catalyst materials were investigated using cyclic voltammetry (CV) in 0.1 M $HClO_4$. CV curves before and after ADT, which involved subjecting the catalyst to 3000 potential cycles between 0.05 and 1.5 V versus RHE, are shown for PtNW/SG, PtNW/G, and commercial Pt/C in **Figure 2**a–c, respectively. It should be noted that the ADT conditions employed are very harsh and include the potential regions in which repeated Pt oxidation/reduction and carbon corrosion will occur.[13] After ADT, additional redox peaks appear in the range of 0.50 to 0.75 V versus RHE. These peaks likely arise due to the formation of quinone/hydroquinone redox species under the high potentials encountered during ADT. The ECSA of the various catalysts was calculated by integrating the hydrogen adsorption–desorption region[14] with ECSA values of 24.5, 24.0 and 53 $m^2\ gm_{Pt}^{-1}$ determined for PtNW/SG, PtNW/G, and Pt/C, respectively. The reduced ECSA of PtNW/SG and PtNW/G in comparison to Pt/C is to be expected, owing to the thicker diameter and anisotropic structure that results in a lower degree of Pt–atom exposure.[2,15] Normalized ECSA values obtained after a varying number of ADT cycles are shown in Figure 2d. It can be seen that after 3000 cycles, PtNW/SG loses only 42% of its initial ECSA, whereas the losses in ECSA for PtNW/G and Pt/C are 72% and 99%, respectively. These results exemplify the excellent stability of PtNW/SG in comparison to PtNW/G and commercial Pt/C under the harsh potentiodynamic conditions of ADT. In our previous study,[9] we found that Pt nanoparticle ECSA losses could also be significantly mitigated using SG supports, owing to the strengthened adsorptive and cohesive interactions induced by sulfur dopant atoms on Pt atoms and nanoclusters, respectively. The current results indicate a similar effect in PtNW/SG based on the significant improvements in ECSA retention observed in comparison to PtNW/G. To investigate the impact of nanostructure control (i.e., nanowires), the as-prepared PtNW/G was compared with Pt nanoparticles supported on undoped graphene (PtNP/G). Electrochemical testing results provided in Figure S5 (Supporting Information) demonstrate that PtNW/G shows clear stability enhancements in comparison to PtNP/G, albeit not to the extent observed in the presence of sulfur doping. This stability enhancement could likely arise owing to surface of the PtNWs that consists primarily of (111) facets, the most thermodynamically favorable configuration, as the (111) planes possess the lowest surface energy of all the low-index crystallographic planes of Pt.[1a]

The ORR activity of PtNW/SG before and after ADT was investigated in oxygen saturated 0.1 M $HClO_4$. Initially at 0.9 V versus RHE, an improved Pt-based mass activity of 167 mA mg_{Pt}^{-1} was observed for PtNW/SG in comparison to PtNW/G (132 mA mg_{Pt}^{-1}) and commercial Pt/C (125 mA mg_{Pt}^{-1}). Moreover, PtNW/SG showed a very high specific activity of 0.675 mA $cm^{-2}{}_{Pt}$ (**Figure 3**d-inset), approaching the U.S. Department of Energy (DOE) target of 0.720 mA $cm^{-2}{}_{Pt}$[16] while PtNW/G and Pt/C demonstrated specific activity values of 0.543 and 0.250 mA $cm^{-2}{}_{Pt}$, respectively. This specific activity enhancement is attributed to the preferential exposure of the (111) facet of the PtNWs that provides higher activity than the (100) facets[17] that are abundant in nanoparticle configurations.[1a] Additionally, the 1D-extended nanostructure of the PtNWs leads to a reduced fraction of defect, step and edge sites that bond spectator species (OH_{ad})

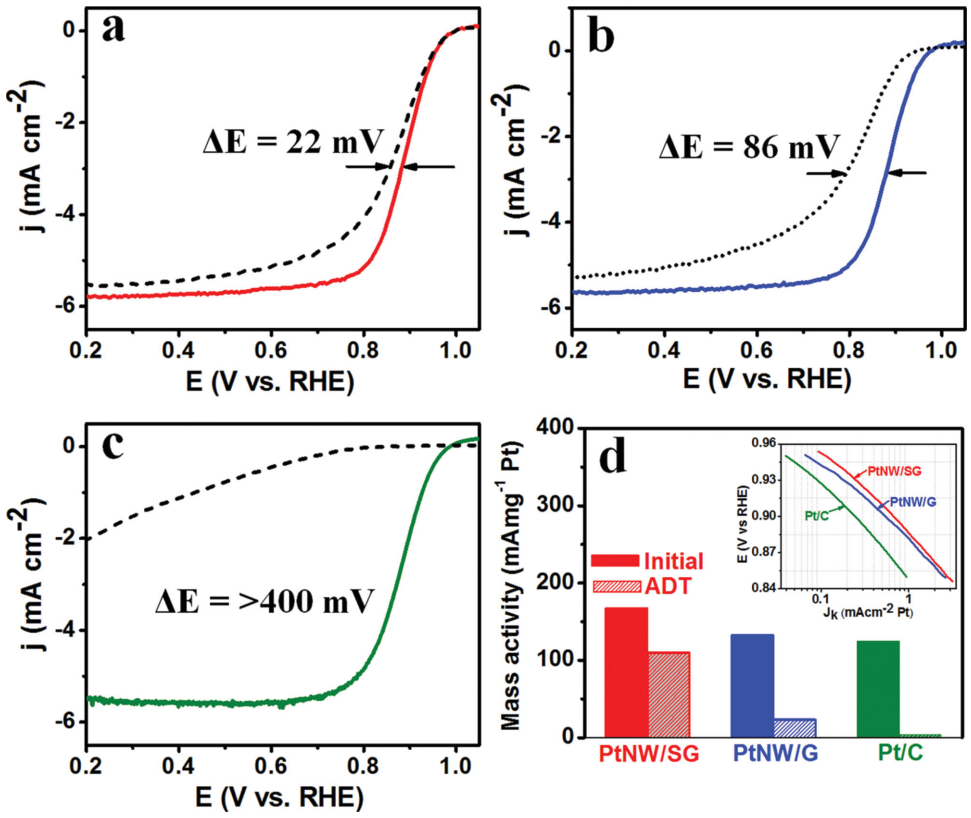

Figure 3. ORR polarization curves of a) PtNW/SG, b) PtNW/G, and c) Pt/C before and after ADT. d) Pt-mass activity and (inset) specific activity comparison.

too strongly, thereby impeding the ORR kinetics.[17c,18] On the other hand, it is very likely that the improved activity of PtNW/SG in comparison to PtNW/G arises due to the beneficial catalyst-support interactions occurring between Pt and the sulfur dopants present in SG.[9]

Polarization curves obtained before and after ADT are shown in Figure 3a–c for PtNW/SG, PtNW/G, and Pt/C, respectively. After ADT, PtNW/SG shows only a 22 mV loss in half-wave potential, significantly better than the 86 mV half-wave potential loss for PtNW/G and almost complete loss of performance for commercial Pt/C. A comparison of Pt-based mass activities before and after ADT is given in Figure 3d. Notably, PtNW/SG demonstrated a mass activity of 112 mA mg_{Pt}^{-1} at 0.9 V versus RHE after ADT, representing 67% of its initial activity. PtNWG and Pt/C on the other hand showed mass activity values of 22 and 0.5 mA mg_{Pt}^{-1} following ADT, corresponding to only 17% and < 1% of their initial activity, respectively. We additionally investigated the stability of PtNW/SG using the DOE-recommended durability testing protocol that involves 30 000 potential cycles between 0.6 and 1.0 V versus RHE in O_2 saturated 0.1 M $HClO_4$ solution.[4,5d,19] Once again, the ECSA and ORR activity retention of PtNW/SG was superior to that of commercial Pt/C (Figure S6, Supporting Information). Following this testing, the ECSA retention for PtNW/SG and Pt/C were approximately 65% and 33%, respectively, and the losses in half-wave potential were approximately 50 and 250 mV, respectively. Moreover, we collected CV curves of PtNW/SG after 6000 cycles (Figure S6-inset, Supporting Information) and observed only a 12% loss in ECSA. This is a significant improvement over the 30% ECSA loss observed by Lim et al.[20] for unique Pd–Pt nanodendrites after only 4000 cycles, although with a slightly higher upper potential limit (0.6–1.1 V vs RHE). Our results are in more close agreement with the results of Ruan et al.[2a] reporting an ECSA loss of 14.2% after 6000 cycles for ultrathin Pt nanowire networks, although the Pt mass and specific activities of our PtNW/SG were significantly higher (16% and 385%, respectively).

Since the performance degradation of electrocatalyst materials is an important issue, we investigated the morphological and structural changes of the catalysts following ADT. After 3000 cycles, PtNWs were still observed anchored on the surface of SG (**Figure 4**a) with retained crystallographic orientation in the <111> direction (Figure 4b). An energy dispersive spectroscopy (EDS) elemental map of PtNW/SG after ADT is shown in Figure 4c, demonstrating the locations of carbon, sulfur, and platinum species. To avoid interference of the sulfonate species present in nafion, a binder free ADT test was conducted for the purpose of elemental mapping. Interestingly, sulfur atoms are consistently observed to be well distributed along the lengths of the PtNWs, providing indication that these sulfur species serve as anchors to adhere the nanowires to the surface of the SG.[21] This is supported by our recent findings through an ab initio approach that highlighted stronger adsorption of Pt on SG (–2.68 eV) compared with pure graphene (–2.01 eV), and an enhanced Pt nanoparticle cohesive energy of –3.95 eV versus –3.67 eV, respectively.[9] For full details of the Density Functional

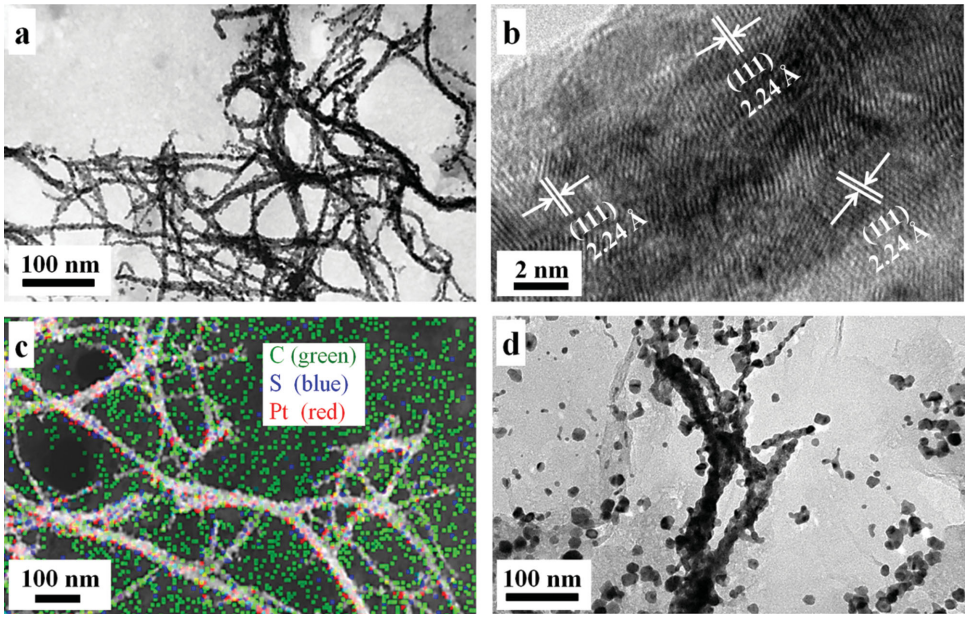

Figure 4. a,b) TEM images and c) EDS mapping of PtNW/SG after ADT. d) TEM image of PtNW/G after ADT.

Theory (DFT) calculations, please refer to the previously published manuscript and supporting information.[9] On the other hand, the structure of PtNW/G was more vulnerable to ADT conditions, with PtNW degradation and aggregation observed, along with the formation of nanoparticle agglomerates on the graphene surface (Figure 4d). The harsh ADT conditions also had a significantly detrimental effect on the structure of Pt/C (Figure S7, Supporting Information), demonstrating dramatic Pt nanoparticle growth and agglomeration.

In conclusion, SG was prepared as a support for the direct growth of platinum nanowires. The growth mechanism of Pt nanowires on SG was investigated and it was found that nanowires are comprised of numerous single crystalline nanoparticles attached and oriented along the <111> crystallographic direction. Notably, PtNW/SG exhibited excellent electrochemical ORR activity and stability in comparison with PtNW/G and commercial Pt/C catalysts under harsh, potentiodynamic conditions. After 3000 cycles of ADT, PtNW/SG retained 58% of its initial ECSA, superior to the only 28% and 1% retained for PtNW/G and commercial Pt/C, respectively. Additionally, PtNW/SG retained 67% of the Pt-based mass activity, whereas the mass activity retention for PtNW/G and commercial Pt/C were 17% and < 1%, respectively. PtNW/SG also exhibited increased Pt-mass-based activity, and an excellent specific activity of 0.675 mA cm^{-2}_{Pt}, approaching the DOE-recommended target of 0.720 mA cm^{-2}_{Pt}.

Experimental Section

Preparation of S-doped Graphene (SG): 100 mg of graphene oxide prepared by a modified Hummer's method was mixed with 100 mg of phenyl disulfide (PDS) by grinding. The materials were loaded into a tube furnace and kept outside the heating zone until the furnace temperature reached 1000 °C. The sample was then slid into the heating zone where it remained for 30 min under argon protection, followed by cooling to room temperature. Graphene was prepared under identical conditions without PDS.

Preparation of S-doped Graphene Supported Platinum Nanowires (PtNW/SG): 9.2 mg of SG was dispersed by 2 h of ultrasonication in a mixture of 12 mL ethylene glycol and 18 mL of *N,N*-dimethyl formaide. 30 mg of $H_2PtCl_6.6H_2O$ was then added followed by the addition of 1.5 g KOH and stirring overnight. The final solution was transferred to a 40 mL Teflon-lined autoclave and heated at 170 °C for 8 h. The resultant black product was collected and washed thoroughly with ethanol and DDI water before drying in a vacuum oven at 80 °C. The same procedure was applied to prepare PtNW/G, with a platinum loading of 50 wt% achieved for both materials.

Materials Characterization: The catalyst materials were characterized using scanning electron microscopy (SEM, LEO FESEM 1530), TEM (JEOL 2010F) equipped with EDS, and XRD (XRG 3000) using monochromatic Cu KA X-rays.

Electrochemical Characterization: 1.75 mg of catalyst materials were dispersed in a solution of 1.9 mL ethanol and 0.1 mL 5 wt% nafion and dropcasted on a glassy carbon electrode to achieve a loading of 22 μg cm^{-2}. CV curves were collected at 50 mV s^{-1} in N_2-saturated 0.1 M $HClO_4$ and ORR measurements at 5 mV s^{-1} under O_2 saturation with electrolyte resistance correction applied. To improve the dispersion of nanowire catalyst on the electrode, 20 wt% carbon black (Vulcan XC-72) was added to the suspension.

Supporting Information

Supporting Information is available from the Wiley Online Library or from the author.

Acknowledgements

This work was financially supported by the NSERC, the University of Waterloo, and the Waterloo Institute for Nanotechnology. This research was conducted as part of the Catalysis Research for Polymer Electrolyte Fuel Cells (CaRPE FC) Network administered from Simon Fraser University and supported by Automotive Partnership Canada (APC) Grant APCPJ 417858-11 through the Natural Sciences and Engineering

Research Council of Canada (NSERC). TEM imaging was conducted at the Canadian Center for Electron Microscopy (CCEM) located at McMaster University (Hamilton, ON).

Received: September 25, 2014
Revised: October 27, 2014
Published online: November 22, 2014

[1] a) Y. H. Bing, H. S. Liu, L. Zhang, D. Ghosh, J. J. Zhang, *Chem. Soc. Rev.* **2010**, *39*, 2184; b) I. E. L. Stephens, A. S. Bondarenko, U. Gronbjerg, J. Rossmeisl, I. Chorkendorff, *Energy Environ. Sci.* **2012**, *5*, 6744.

[2] a) L. Y. Ruan, E. B. Zhu, Y. Chen, Z. Y. Lin, X. Q. Huang, X. F. Duan, Y. Huang, *Angew. Chem. Int. Ed.* **2013**, *52*, 12577; b) S. H. Sun, G. X. Zhang, D. S. Geng, Y. G. Chen, R. Y. Li, M. Cai, X. L. Sun, *Angew. Chem. Int. Ed.* **2011**, *50*, 422.

[3] a) Z. W. Chen, M. Waje, W. Z. Li, Y. S. Yan, *Angew. Chem. Int. Ed.* **2007**, *46*, 4060; b) S. J. Guo, S. Zhang, D. Su, S. H. Sun, *J. Am. Chem. Soc.* **2013**, *135*, 13879.

[4] United States Department of Energy: Technical Plan – Fuel Cells (2012), http://www1.eere.energy.gov/hydrogenandfuelcells/mypp/pdfs/fuel_cells.pdf, (accessed: November 2013).

[5] a) S. M. Alia, K. Jensen, C. Contreras, F. Garzon, B. Pivovar, Y. S. Yan, *ACS Catal.* **2013**, *3*, 358; b) S. J. Guo, D. G. Li, H. Y. Zhu, S. Zhang, N. M. Markovic, V. R. Stamenkovic, S. H. Sun, *Angew. Chem. Int. Ed.* **2013**, *52*, 3465; c) D. C. Higgins, S. Y. Ye, S. Knights, Z. W. Chen, *Electrochem. Solid-State Lett.* **2012**, *15*, B83; d) C. Koenigsmann, A. C. Santulli, K. P. Gong, M. B. Vukmirovic, W. P. Zhou, E. Sutter, S. S. Wong, R. R. Adzic, *J. Am. Chem. Soc.* **2011**, *133*, 9783.

[6] a) S. H. Sun, F. Jaouen, J. P. Dodelet, *Adv. Mater.* **2008**, *20*, 3900; b) S. H. Sun, G. X. Zhang, D. S. Geng, Y. G. Chen, M. N. Banis, R. Y. Li, M. Cai, X. L. Sun, *Chem.-Eur. J.* **2010**, *16*, 829; c) S. H. Sun, G. X. Zhang, Y. Zhong, H. Liu, R. Y. Li, X. R. Zhou, X. L. Sun, *Chem. Commun.* **2009**, 7048.

[7] V. Chabot, D. Higgins, A. P. Yu, X. C. Xiao, Z. W. Chen, J. J. Zhang, *Energy Environ. Sci.* **2014**, *7*, 1564.

[8] a) J. E. Park, Y. J. Jang, Y. J. Kim, M. S. Song, S. Yoon, D. H. Kim, S. J. Kim, *Phys. Chem. Chem. Phys.* **2014**, *16*, 103; b) Z. Yang, Z. Yao, G. F. Li, G. Y. Fang, H. G. Nie, Z. Liu, X. M. Zhou, X. Chen, S. M. Huang, *ACS Nano* **2012**, *6*, 205.

[9] D. Higgins, M. A. Hoque, M. H. Seo, R. Wang, F. Hassan, J.-Y. Choi, M. Pritzker, A. Yu, J. Zhang, Z. Chen, *Adv. Funct. Mater.* **2014**, *24*, 4325.

[10] B. Y. Xia, H. B. Wu, Y. Yan, X. W. Lou, X. Wang, *J. Am. Chem. Soc.* **2013**, *135*, 9480.

[11] a) D. S. Li, M. H. Nielsen, J. R. I. Lee, C. Frandsen, J. F. Banfield, J. J. De Yoreo, *Science* **2012**, *336*, 1014; b) Z. Y. Tang, N. A. Kotov, *Adv. Mater.* **2005**, *17*, 951.

[12] D. Azulai, E. Cohen, G. Markovich, *Nano Lett.* **2012**, *12*, 5552.

[13] X. Xie, Y. Xue, L. Li, S. Chen, Y. Nie, W. Ding, Z. Wei, *Nanoscale* **2014**, *6*, 11035..

[14] C. Higgins, D. Meza, Z. W. Chen, *J. Phys. Chem. C* **2010**, *114*, 21982.

[15] H. W. Liang, X. A. Cao, F. Zhou, C. H. Cui, W. J. Zhang, S. H. Yu, *Adv. Mater.* **2011**, *23*, 1467.

[16] L. Su, S. Shrestha, Z. H. Zhang, W. Mustain, Y. Lei, *J. Mater. Chem. A* **2013**, *1*, 12293.

[17] a) N. Markovic, H. Gasteiger, P. N. Ross, *J. Electrochem. Soc.* **1997**, *144*, 1591; b) D. F. van der Vliet, C. Wang, D. Tripkovic, D. Strmcnik, X. F. Zhang, M. K. Debe, R. T. Atanasoski, N. M. Markovic, V. R. Stamenkovic, *Nat. Mater.* **2012**, *11*, 1051; c) J. L. Zhang, M. B. Vukmirovic, Y. Xu, M. Mavrikakis, R. R. Adzic, *Angew. Chem. Int. Ed.* **2005**, *44*, 2132.

[18] a) J. Greeley, I. E. L. Stephens, A. S. Bondarenko, T. P. Johansson, H. A. Hansen, T. F. Jaramillo, J. Rossmeisl, I. Chorkendorff, J. K. Norskov, *Nat. Chem.* **2009**, *1*, 552; b) V. R. Stamenkovic, B. Fowler, B. S. Mun, G. F. Wang, P. N. Ross, C. A. Lucas, N. M. Markovic, *Science* **2007**, *315*, 493; c) I. E. L. Stephens, A. S. Bondarenko, F. J. Perez-Alonso, F. Calle-Vallejo, L. Bech, T. P. Johansson, A. K. Jepsen, R. Frydendal, B. P. Knudsen, J. Rossmeisl, I. Chorkendorff, *J. Am. Chem. Soc.* **2011**, *133*, 5485.

[19] Y. Kim, J. W. Hong, Y. W. Lee, M. Kim, D. Kim, W. S. Yun, S. W. Han, *Angew. Chem. Int. Ed.* **2010**, *49*, 10197.

[20] B. Lim, M. J. Jiang, P. H. C. Camargo, E. C. Cho, J. Tao, X. M. Lu, Y. M. Zhu, Y. N. Xia, *Science* **2009**, *324*, 1302.

[21] R. Y. Wang, D. C. Higgins, M. A. Hoque, D. Lee, F. Hassan, Z. W. Chen, *Sci. Rep.-UK* **2013**, *3*, 2431.